Microwave Atmospheric Temperature Sounding: Effects of Clouds on the Nimbus 5 Satellite Data

D. H. STAELIN, A. L. CASSEL, K. F. KUNZI,[1] R. L. PETTYJOHN, R. K. L. POON[2] AND P. W. ROSENKRANZ

Research Laboratory of Electronics, Massachusetts Institute of Technology, Cambridge 02139

J. W. WATERS

Jet Propulsion Laboratory, California Institute of Technology, Pasadena 91103

(Manuscript received 11 September 1974, in revised form 4 June 1975)

ABSTRACT

The microwave spectrometer on the Nimbus 5 earth observatory satellite has been used to measure thermal radiation in five frequency bands between 22.235 and 58.8 GHz. Clouds were observed to affect less than 0.5% of the temperature profile soundings. Most such effects occur in the intertropical convergence zone and alter the inferred temperature profile by less than a few degrees Centigrade. These effects are evident as cold spots at 53.65 GHz and can be identified by virtue of their small spatial extent, in contrast to smooth variations characteristic of normal atmospheric temperature fields. These effects at 53.65 GHz are sufficiently well correlated with inferred liquid water abundances that they can be used for detecting major storm systems over both land and sea.

1. Introduction

Since launch on 11 December 1972 the Nimbus 5 (Nimbus E) Microwave Spectrometer (NEMS) has been making passive microwave measurements of global atmospheric temperature profiles as well as measurements of atmospheric water content and other geophysical parameters. Preliminary NEMS results were reported by Staelin *et al.* (1973) and earlier aircraft observations with NEMS were discussed by Rosenkranz *et al.* (1972). The general principles of remote sensing with passive microwave techniques have been reviewed elsewhere (Staelin, 1969).

The five-channel NEMS was fabricated at the California Institute of Technology Jet Propulsion Laboratory. It views nadir with half-power antenna beamwidths of 10° and measures thermal radiation emitted by the terrestrial atmosphere and surface. Individual channels are located on a weak water vapor resonance, in a spectral window, and at three positions on the edge of an oxygen absorption band; the center frequencies of channels 1–5 are 22.235, 31.4, 53.65, 54.9 and 58.8 GHz, respectively. The satellite moves in a nearly circular sun-synchronous orbit at an inclination of 80° and an altitude of 1096 km. Equator crossings occur near local noon and midnight.

2. Effects of clouds on temperature profile measurements

A major purpose of the NEMS experiment is to evaluate passive microwave techniques for use on operational meteorological and geophysical satellites. One principal uncertainty was the ability of NEMS to obtain meaningful atmospheric soundings in the presence of clouds, particularly in regions of total overcast which infrared sensors cannot penetrate.

Channels 3, 4 and 5 respond primarily to the atmospheric temperature profile. The microwave emission spectrum is related to the temperature profile because at each frequency the thermal radiation received originates from a specific atmospheric layer approximately 10 km thick, as was first noted by Meeks and Lilley (1963). The average atmospheric temperature of each layer equals the brightness temperature of radiation incident upon the satellite at the frequency of interest. The radiation measured in channels 3, 4 and 5 originates in layers centered near 4, 11 and 18 km, respectively. A more complete discussion of the temperature profile observations is contained in the accompanying paper by Waters *et al.* (1975).

Only channel 3, which penetrates the atmosphere more deeply than the other two temperature-sounding channels, is measurably affected by clouds. Heavy clouds at altitudes of several kilometers or more can appear as cold spots in the channel 3 data because such clouds are normally colder than the brightness temperature T_B of the radiation incident upon the cloud from below and thus reduce the T_B observed by NEMS. Channels 4 and 5 are not affected because they sense atmospheric layers located above most heavy clouds.

Cloud opacity depends upon frequency ν, cloud temperature T, and the drop size distribution. For small

[1] Present affiliation: Institute of Applied Physics, University of Berne, Switzerland.

[2] Present affiliation: Department of Electronics, Chinese University of Hong Kong.

water drops characteristic of non-precipitating clouds, i.e., drop radius $\lesssim 50$ μm, the absorption in this wavelength region is approximately $3.55\times10^{-3-(T/82)}M\lambda^{-2}$ [cm^{-1}], where M is the liquid water density of the clouds (g m^{-3}), λ is wavelength (cm), and T is cloud temperature (K), as deduced from data presented by Goldstein (1951).

Ice clouds such as cirrus are generally negligible in comparison because such clouds are typically less dense and because ice absorbs microwave radiation much less strongly than water. In fact, most clouds heavy enough to absorb significant radiation near 1 cm wavelength are also raining. The best measurements of such absorption by clouds have been systematic microwave observations of solar or sky brightness temperatures over one or more years from fixed locations. Studies at mid-latitudes by Wilson (1969), Davies (1973) and Hogg (1973) all suggest that zenith attenuation near 1 cm wavelength exceeds 3 dB and 10 dB approximately 1% and 0.1–0.01% of the time, respectively. Attenuation values observed by Davies in Slough, England, were somewhat lower, and those observed by Hogg and Wilson in Holmdel, N. J., were somewhat higher.

If the attenuating portions of the clouds were predominantly below ~4 km altitude or if they were distributed in small isolated cells over a wide area, then the clouds would have an effect less than 1 K on channel 3. On the other hand, if the attenuating portions of the clouds were largely above 4 km altitude or contained in tightly packed cells clustered in weather systems comparable in size to the NEMS field of view, i.e., 200 km, then the effects of clouds on channel 3 of NEMS could be 5 or 10 K. One of the major results sought by the NEMS experiment was the true impact of clouds on channel 3 and hence the statistical character of atmospheric liquid water at various latitudes and seasons.

The observed sensitivity of NEMS channel 3 to clouds and other influences, such as the terrestrial surface, is indicated in Fig. 1 where the observed T_B of channel 3 is plotted for six typical traverses of the equator by NEMS on 23 December 1972. Each traverse is centered near the equator where atmospheric temperature variations are minimum. The variations in observed brightness temperature represent the sum of actual atmospheric temperature variations plus the effects of heavy clouds and surface variations. In traverses (a), (b) and (c) the peak-to-peak variation is about 2 K, most of which is associated with large-scale weather systems. The rms radiometer noise is approximately 0.1 K for each 16 s sample and thus accounts for much of the noise. In 16 s the satellite moves 100 km. In three other traverses the effect of the terrestrial surface is evident as NEMS crossed ocean-land boundaries. In (d) the abrupt increase of 1.5 K occurred as NEMS passed from ocean over the Mexican coast

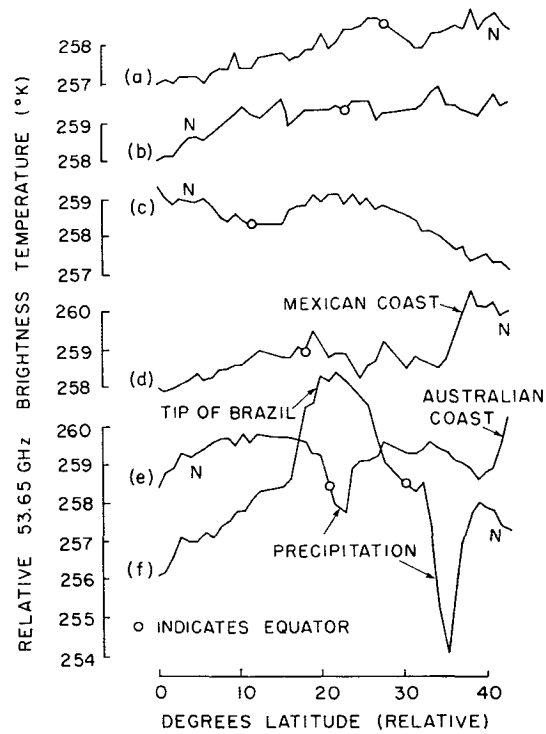

FIG. 1. Relative brightness temperatures at 53.65 GHz for six equator crossings on 23 December 1972. The northern end of each scan is indicated by N, and the equator crossings are marked by circles. Equator crossings occur at longitudes 13.5°W, 126.2°E, 72.5°E, 94.1°W, 153.0°E, and 40.5°W for crossings (a)–(f), respectively.

near Acapulco. In (e) a similar increase at the end occurred over the coast of Australia, and in (f) the increase near the equator occurred over Brazil. These changes in brightness temperature arise because sea water has an emissivity of approximately 0.5, less than the 0.8–1.0 emissivity of most land. This effect is of little consequence to most temperature soundings because channels 1 and 2 of NEMS yield the effective surface emissivity with sufficient accuracy that this effect can be compensated when determining the temperature profiles.

The effects of heavy clouds appear in (e) and (f) as local minima in brightness temperature of 1.5 and 4 K, respectively; each minimum spans approximately 3° latitude.

If the obvious effect of land-sea transitions and heavy clouds are deleted from the 53.65 GHz brightness temperature traces in Fig. 1, then the remaining traces, which contain effects of ordinary weather systems, are remarkably stable and unperturbed over long distances even in the presence of a wide variety of ordinary clouds. This stability over long distances should permit horizontal atmospheric temperature differences, averaged over layers several kilometers thick, to be determined with accuracies of a few tenths of a degree

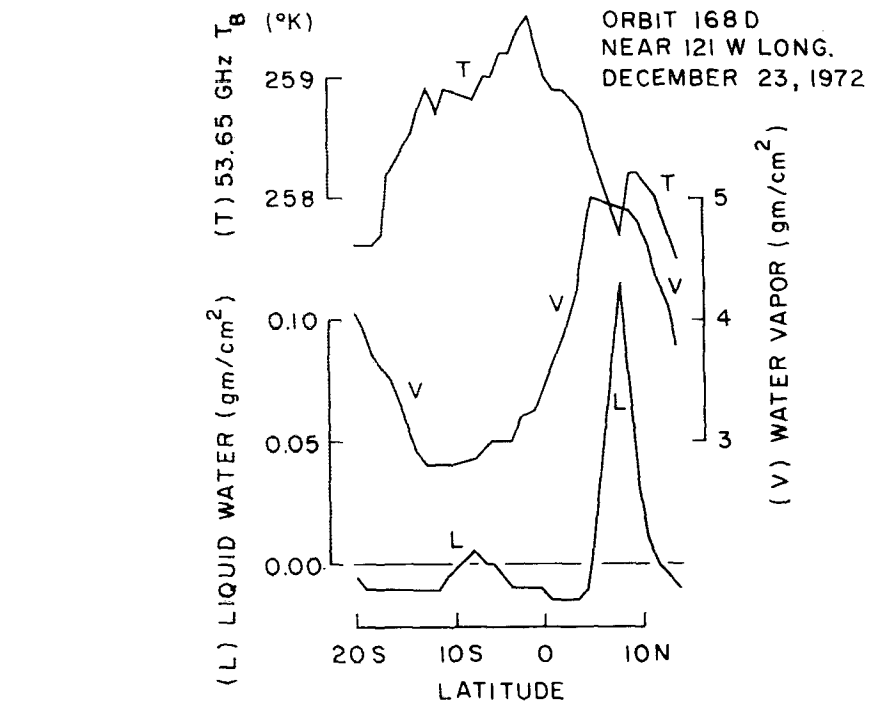

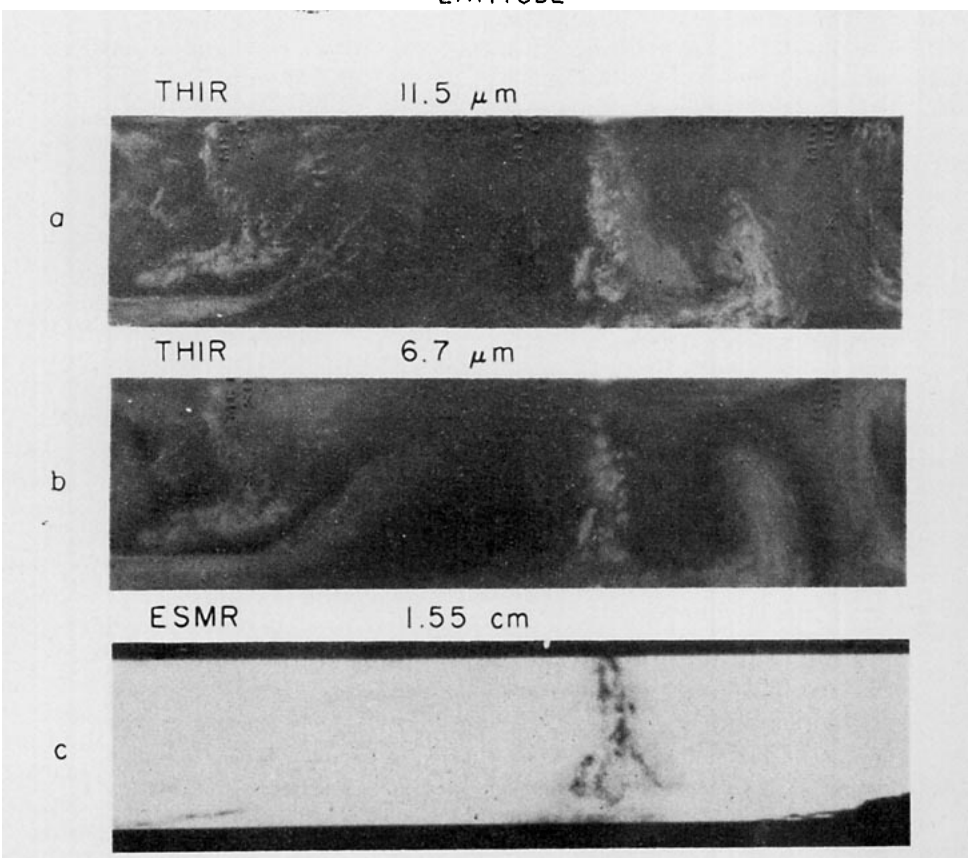

FIG. 2. Comparison of NEMS-inferred values of water vapor and liquid water with the 53.65 GHz brightness temperature, the THIR 11.5 and 6.7 μm images, and the ESMR 1.55 cm image, as a function of latitude for orbit 168 near 121°W longitude, 23 December 1972.

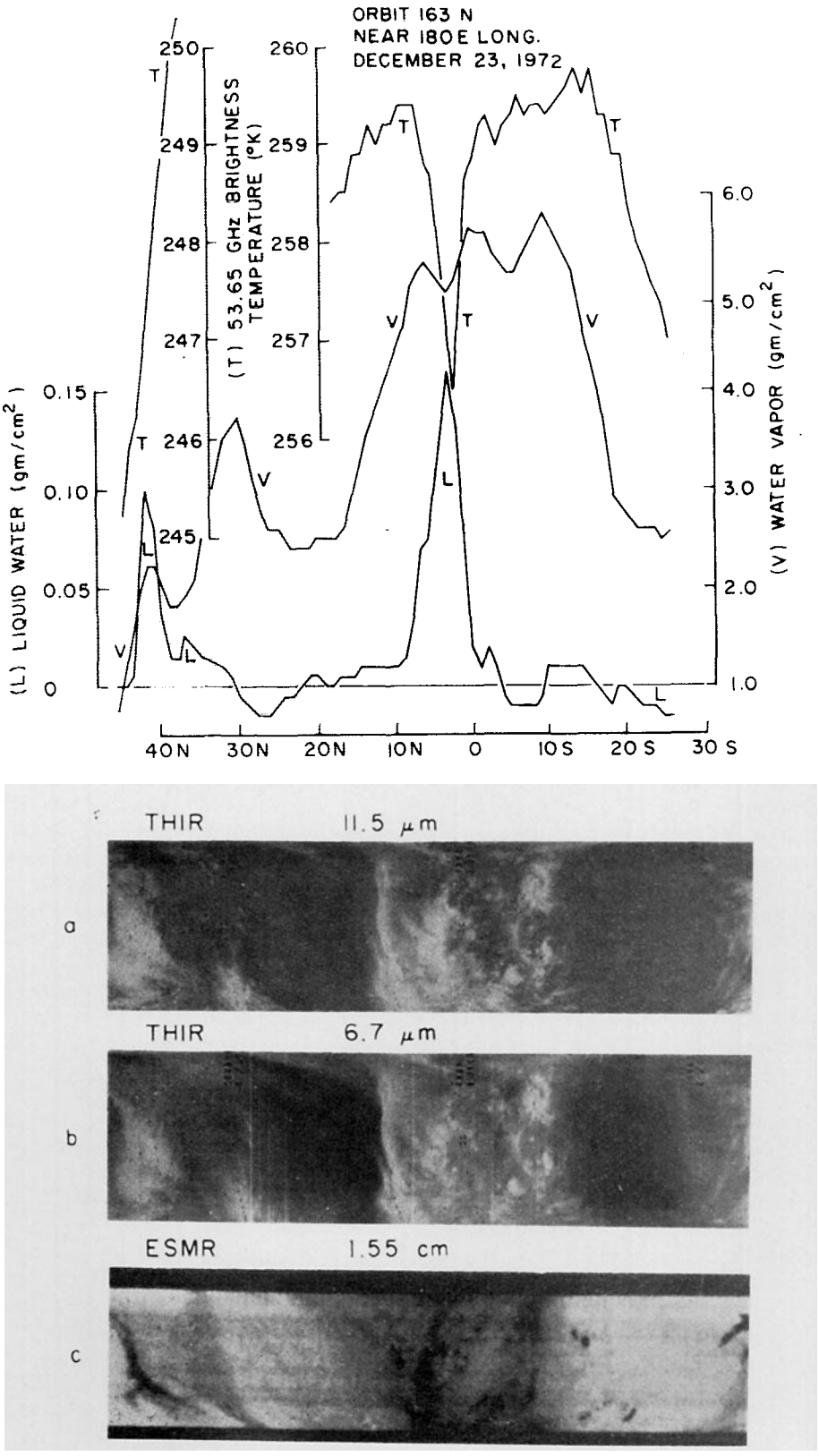

FIG. 3. As in Fig. 2 except for orbit 163 near 180°E longitude, 23 December 1972.

TABLE 1. Number of 53.65 GHz T_B minima as a function of amplitude and location.

Amplitude (K)	Ocean Latitude range			Land Latitude range		
	0°–15°	15°–50°	>50°	0°–15°	15°–50°	>50°
1.0–1.5	17	7		15	14	7
1.5–2.0	5	2		3	3	1
2.0–2.5	1	1		3	3	
2.5–3.0	1					1
3.0–3.5				1		
3.5–4.0	1					
4.0–4.5						
4.5–5.0					1	
Total number	25	10	0	22	21	9
Percent of 20,000		0.17			0.25	
Total percent of 20,000			0.42			

Kelvin, except when very heavy clouds with densities exceeding $\sim$0.05 g cm^{-2} are present.

The nature of these cloud-induced depressions of brightness temperature can be seen more clearly in Figs. 2 and 3, which contain 53.65 GHz brightness temperature data together with 1) the corresponding values of integrated water vapor and liquid water (g cm^{-2}) inferred from channels 1 and 2 of NEMS, 2) the simultaneous 11.5 μm THIR (Temperature, Humidity Infrared Radiometer) window channel infrared image, 3) the 6.7 μm THIR water vapor infrared image, and 4) the 1.55 cm wavelength ESMR (Nimbus 5 Electrically Scanned Microwave Radiometer) image. The NEMS-inferred abundances of water vapor and liquid water have rms accuracies of $\sim$0.3 and $\sim$0.015 g cm^{-2}, respectively, and were determined by a linear statistical regression technique similar to that described by Rosenkranz *et al.* (1972).

Figs. 2 and 3 illustrate the effects of the intertropical convergence zone (ITCZ) upon channel 3. Although clouds are evident in a range of latitudes, channel 3 appears locally cooler only at the center of the ITCZ, marked by cold high-altitude clouds in the THIR images, and by the black rain band in the ESMR image. The water vapor content inferred from NEMS shows a band of humid air, in which the channel 3 brightness minimum due to clouds is located, coincident with the peak in NEMS-inferred liquid water. These figures are consistent with the prediction of Rosenkranz *et al.* that a uniform heavy cloud containing approximately 0.1 g cm^{-2} liquid water, if centered near 5 km altitude, would produce approximately a 1.5 K minimum in brightness temperature over ocean. Note that clouds present when the NEMS liquid water content is low have no observable effect upon the 53.65 GHz brightness temperature.

Fig. 3 contains both the ITCZ and, at 42°N, an occluded front. Although the frontal system contains nearly as much liquid water as the ITCZ, it produces no minimum in the sharp thermal gradient, whereas the ITCZ minimum is 2.5 K. In theory (Rosenkranz *et al.*, 1972), the effect of a given amount of atmospheric liquid water generally increases with increasing cloud altitudes greater than $\sim$3 km over ocean or 0 km over land. Thus the reduced effect of the occluded front is probably due to its lower average altitude.

A computer search for 53.65 GHz T_B minima was conducted for 8–13 February 1973 (orbits 789–861) and 28 February through 6 March, 1973 (orbits 1077–1157). Both hemispheres were examined, so both summer and winter data were included. The minima were identified by examining each 16 s sample and requiring that each sample n be 1) a local minimum, 2) more than 0.3 K below both samples $n+2$ and $n-2$, and 3) 1 K or more below the average of samples $n+2$, $n-2$. Thus minima of 200–300 km diameter were sought. Experiments were performed with different definitions of T_B minima, e.g., the difference between a sample n and the averages of either samples $n\pm2$ or $n\pm3$. The definition used here which involved samples n and $n\pm2$, was sufficiently limited spatially to be reasonably unaffected by normal atmospheric temperature variations, but was still sufficiently wide to be quite sensitive to most clouds. The use of different reasonable definitions for T_B minima might vary the statistics by a factor of 2, the differences mainly concerning the identification of minima of 1.5 K or less.

In Table 1 the number of minima found is listed separately for land and sea as a function of amplitude and latitude. Approximately 40,000 16 s samples might have contained a T_B minimum, and since each minimum typically is 1–3 samples wide, $\sim$20,000 independent samples were examined. Over ocean the great majority of minima are within 15° latitude of the equator, and are generally associated with the ITCZ. Only four cases (0.02%) are greater than 2 K.

Over land there are slightly more and somewhat larger minima, which are more evenly divided between equatorial and other regions. The fact that T_B minima due to clouds over land are slightly larger than those over ocean is consistent with the analysis of Rosenkranz *et al.* (1972). The largest T_B minimum found, 4.7 K, was associated with a major storm over northeast Argentina. The land samples were restricted to regions where the general surface elevation was less than 1 km, because mountains such as the Andes can also produce minima of comparable magnitude.

Some of the minima are due to real variations in atmospheric temperature. One case involved a very narrow tongue of cloudless cold arctic air between two warm tropical air masses; such minima constitute less than 5–10% of the total. In major storm systems it is difficult to determine whether the T_B minimum is due to clouds or to storm temperature structure. Much of the effect is probably due to liquid water absorption rather than to temperature anomalies, however, since the results are quite consistent with those anticipated for liquid water clouds alone. Furthermore, the temperature structure required to produce the observed

TABLE 2. Changes in inferred temperature profile over ocean caused by a 1 K decrease in T_B (53.65 GHz).

Altitude (mb)	Decrease (K)
1000	−2.29
850	−1.90
700	−1.54
500	−1.09
400	−0.30
300	+0.35
250	+0.90
200	+0.84
150	+0.50
100	−0.08
70	−0.33
50	−0.60
30	−0.68

effect, i.e., a colder troposphere, is not commonly expected. With our present approximately linear statistical scheme for determining atmospheric temperature, the impact of a 1 K 53.65 GHz T_B minimum on the inferred profile is as presented in Table 2. The procedure for determining temperature profiles is discussed by Waters *et al.* (1975).

The maximum effect is 2.29 K at 1000 mb for a T_B minimum of 1 K, and the major effect is at altitudes below 500 mb. Table 1 indicates that only 0.42% of the soundings were affected, and only 0.015% were affected by minima larger than 3°K. Only one large T_B minimum, or 0.005%, occurred outside the ITCZ. The impact of cloud-induced T_B minima on global temperature maps can be reduced further. For example, an algorithm similar to that used here to detect minima could be used to identify and eliminate them. Alternatively they might be compensated over ocean by using the NEMS liquid water and temperature profile measurements to estimate a probable amplitude of the T_B minimum.

3. Water vapor and liquid water contents of clouds that perturb temperature profile measurements

The meteorological character of 53.65 GHz T_B minima was studied further by plotting, as in Fig. 4, the NEMS-inferred atmospheric water vapor and liquid water contents for each T_B minimum over ocean in the data set described earlier. The water contents were inferred by regressing theoretically computed brightness temperatures against the corresponding water contents for an ensemble of radiosondes. Most of the 80 minima larger than 0.5 K are in a cluster having water vapor values between 5 and 6 g cm^{-2}. All of these occur at latitudes within 30° of the equator. The 10 mid-latitude and polar minima, ranging up to 2.5 K, are more sparse and occur at various inferred water vapor values. Two or three of these might be due to causes other than clouds. The amplitude of the T_B minimum is also indicated in the same figure, and it can be seen that larger T_B depressions are associated with heavier clouds.

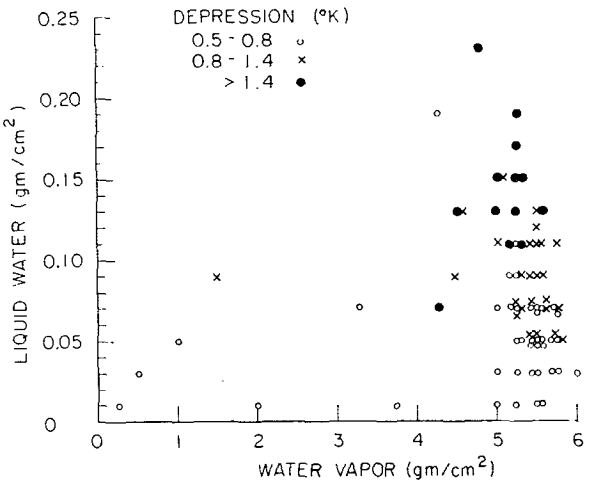

FIG. 4. Depression amplitude at 53.65 GHz over ocean as a function of NEMS-inferred liquid water and water vapor abundances.

The relationship between the amplitudes of the T_B minima and cloud water content is more explicit in Fig. 5, where the size of all the T_B minima of Fig. 4 are replotted as a function of cloud liquid water content. The correlation is as expected from the analysis of Rosenkranz *et al.* for uniform cloud decks at 5 km altitude. The correlation is not perfect, partly because the effective average cloud height varies from cloud to cloud, and because the clouds are not uniform layers but are composed of unresolved clusters of more nearly opaque cloud cells. Such cloud cells are partially resolved in the 1.55 cm wavelength ESMR images contained in Figs. 2 and 3.

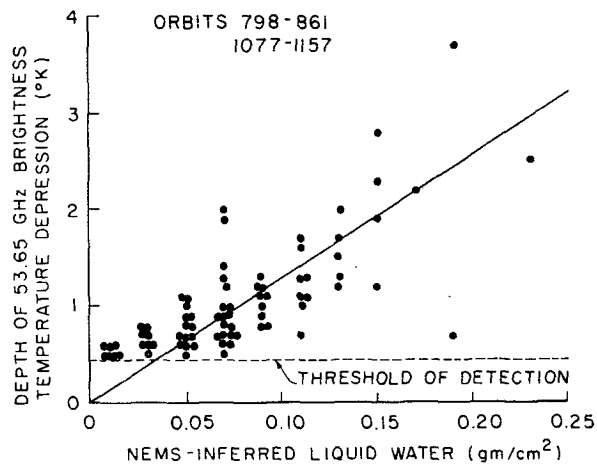

FIG. 5. Correlation between the depth of the 53.65 GHz brightness temperature depression and the corresponding NEMS-inferred liquid water abundances for depressions above the threshold of detection, over ocean.

The implication of Fig. 5 is that the amplitudes of T_B minima could be used as a crude indication of the presence and intensity of large storm systems over both land and sea. The cloud-sensing potential is even greater for channels at slightly more transparent temperature sounding frequencies between 52 and 53.65 GHz. These lower frequencies penetrate still more deeply into the atmosphere from space, thus providing a warmer background signal and hence greater contrast for cloud observations.

It should be noted that the liquid water densities shown in Figs. 4 and 5 are inferred from regression equations based on the assumption that the liquid water is arranged in uniform cloud layers and not in the form of dense cells. This is a good approximation if the most dense cells attenuate less than 3 dB, but if the cells are more opaque than this, the microwave radiometer becomes increasingly blind to their water content. Instead the total area covered by the opaque cells becomes the dominant parameter sensed by the radiometer. The data of Davies, Hogg, and Wilson, noted earlier, suggests that the atmospheric opacity exceeds 3 dB approximately 1% of the time, comparable to the 0.5% of NEMS soundings affected by clouds. Not all dense cells affect NEMS because not all cells are in clusters covering a sufficiently large fraction of the NEMS field of view. Thus the total atmospheric liquid water contents shown in Figs. 4 and 5 are probably underestimated, particularly for the heaviest clouds. This tendency for heavy water concentrations to form in cells also diminishes the effect of such cells on channel 3 because they then cover only a fraction of the field of view. This nonlinear relationship between total liquid water content and the microwave response can be empirically compensated if the statistical distribution of liquid water in clouds is sufficiently constant.

4. Summary and conclusions

Perhaps the most important result is the fact that only 0.5% of all NEMS temperature soundings are measurably affected by clouds, and that most of these soundings occur in the ITCZ. Furthermore, large clouds can usually be detected, and thus should not disrupt numerical weather prediction schemes or other applications of the data. The small temperature gradients observed at 53.65 GHz in the absence of clouds suggest that NEMS can measure such gradients with an accuracy of a few tenths of a degree K over distances of hundreds to thousands of kilometers.

The characteristic small spatial extent of the 53.65 GHz T_B minima enables them to be distinguished from the more slowly varying atmospheric temperature field, and their amplitude is correlated with cloud water content. Therefore such minima can be used to detect the presence and significance of major storm systems over both land and sea. The use of slightly longer wavelengths should enhance this capability.

Acknowledgments. We thank F. T. Barath, J. C. Blinn, III, and E. J. Johnston for their development and preflight calibration of the NEMS instrument, and T. Wilheit and others at the NASA Goddard Space Flight Center for making available the ESMR and THIR images. This work was supported by NASA Contracts NAS7-100 and NAS5-21980.

REFERENCES

Davies, P. G., 1973: Radiometer measurements of atmospheric attenuation at 19 and 37 GHz along sun-earth paths. *Proc. IEEE*, **2**, 159–164.

Goldstein, H., 1951: Attenuation by condensed water. *Propagation of Short Radio Waves*, D. E. Kerr, Ed. McGraw-Hill, 674–677.

Hogg, D. C., 1973: Intensity and extent of rain on earth-space paths. *Nature*, **243**, 337–338.

Meeks, M. L., and A. E. Lilley, 1963: The microwave spectrum of oxygen in the earth's atmosphere. *J. Geophys. Res.* **68**, 1683–1703.

Rosenkranz, P. W., F. T. Barath, J. C. Blinn III, E. J. Johnston, W. B. Lenior, D. H. Staelin and J. W. Waters, 1972: Microwave radiometric measurements of atmospheric temperature and water from an aircraft. *J. Geophys. Res.*, **77**, 5833–5844.

Staelin, D. H., 1969: Passive remote sensing at microwave wavelengths. *Proc. IEEE*, **57**, 427–439.

——, A. H. Barrett, J. W. Waters, F. T. Barath, E. J. Johnston, P. W. Rosenkranz, N. E. Gaut and W. B. Lenoir, 1973: Microwave spectrometer on the Nimbus 5 satellite: Meteorological and geophysical data. *Science*, **182**, 1339–1341.

Waters, J. W., K. F. Kunzi, R. L. Pettyjohn, R. K. L. Poon and D. H. Staelin, 1975: Remote sensing of atmospheric temperature profiles with the Nimbus 5 microwave spectrometer. *J. Atmos. Sci.*, **32**, 1953–1969.

Wilson, R. W., 1969: Arm tracker measurements of attenuation by rain at 16 and 30 GHz. *Bell Sys. Tech. J.*, **48**, 1383–1404.